Design and experiment of corn low damage threshing device based on DEM

Xiaoyu Li[1,2], Yuefeng Du[1,2*], Enrong Mao[1,2], Yan'an Zhang[1,2], Lei Liu[1,2], Dafang Guo[1,2]

(1. *Beijing Key Lab Optimized Design for Modern Agricultural Equipment, China Agricultural University, Beijing 100083, China*;
2. *College of Engineering, China Agricultural University, Beijing 100083, China*)

Abstract: Kernel broken rate is an important index to evaluate the maize kernel direct harvesting quality. In view of the problem of the high kernel broken rate in the present maize harvester, a new threshing cylinder was designed in this study. This device utilized rasp bar to achieve low damaged maize ears threshing. In order to determine the structure and working parameters of threshing device, the "crop-crop" contact model and the "crop-mechanical" interaction system were established and analyzed based on the discrete element method first, and the mathematical expressions of the related kinematic response of maize kernel under the external force were obtained. Then, the structure parameters of rasp bar were studied through EDEM simulation experiment, and the working parameters were determined through test-bed experiment. Finally, the simulation experiment results and test-bed experiment results were verified through field experiment. The results showed that when the threshing cylinder speed was 356 r/min, the concave clearance was 40 mm, the installation distance of rasp bar was 250 mm with 50Mn steel, and the feeding amount was 8 kg/s, the kernel broken rate was 1.93%, which satisfied the requirements of maize harvest standard. This study proved that the DEM (Discrete Element Method) can be adopted to guide the optimization design of mechanical structure, and it has certain value for the research and development of operation equipment of other agricultural crops.
Keywords: DEM, maize threshing, low damage harvesting, kernel broken rate, simulation
DOI: 10.25165/j.ijabe.20231603.7042

1 Introduction

Maize direct harvesting is the best way to harvest maize ears[1]. However, the direct harvesting method inevitably causes damage to the integrity of maize kernel. Therefore, it is of great significance to study low damage threshing equipment to reduce the kernel broken rate. At present, some studies have reported the design of structural and the choice method of working parameters of threshing device, the design cases of threshing device for wheat, rice and other crops provide good references for this study[2-4]. Wang et al.[5] designed a threshing cylinder with gradually changing diameter, which can reduce the collision damage of mechanical structure to ears and increase the contact friction frequency between ears, thus achieving the goal of reducing kernel broken rate. A combined maize threshing and separating device adopted a round head nail tooth to threshing the maize ears, the mechanical changes of maize ears under the impact of nail tooth were analyzed, the experiment results showed that kernel broken rate was reduced to 8.64%, and the

unremoved rate was 0.2%, compared with the traditional threshing device, the threshing performance was improved, but there was still a shortage of high index[6]. Besides, the threshers of flexible hammer-claw with different types were designed, and the optimal combination of working parameters was determined by experiments. Some researchers have optimized the design of threshers, and put forward the rasp bar type and nail-tooth type and so on, but in the laboratory environment, the problem of high kernel broken rate still exists[7]. Although the threshing device mentioned above has promoted the development of maize kernel direct harvesting machinery to a certain extent, the designed machineries were relatively complex, and most of them were still in the laboratory research stage, which was difficult to meet the harsh and changeable working environment. In addition, there was a lack of in-depth research on the interaction system between machinery and maize ears, so the developed machineries have a reliability poor harvesting effect, which are not satisfactory.

Nowadays, with the development of science and technology and computer technology, the application of simulation software in industrial design can help researchers shorten the research and development cycle, improve work efficiency, and greatly liberate productivity and labor, it gradually suppresses the traditional technological production mode. Cundall et al.[8] is the first scholar in the world to put forward the DEM, he regarded matter as a series of discrete particles, and explained the motion state of each particle based on Newton's classical mechanics of motion. So far this method has been widely adopted to study the basic characteristics of granular materials. The interaction between agricultural crops and mechanical devices can be optimized by using discrete element method and EDEM discrete element simulation software, so as to provide guidance for harvester performance optimization, which has

become a hot topic in developing machineries[9-14]. Yu et al.[7,15] established a discrete element model of maize ears based on particle splicing method, developed an embedded maize threshing analysis software, simulated the threshing process of ears, and obtained the influence of threshing cylinder speed and feeding amount on threshing effect from a microscopic point of view. The above research verified the feasibility and effectiveness of using DEM and related software to analyze the operation process of granular materials, which can provide reference for the development of other agricultural crop production machinery.

In this study, the design scheme of threshing cylinder based on discrete element method was put forward, the "crop-machinery" interaction system model was established, and the kinematics law of maize kernel in the threshing process was derived. Due to the selection and determination of some structure parameters of threshing device are difficult to be realized through common experiment means, in this study, the EDEM was utilized to solve this problem. By setting structural parameters, material characteristics, contact parameters, motion parameters and constraint conditions, which were consistent with the real environment, then an accurate result can be calculated. Finally, the performance of the designed threshing device under different working conditions was obtained through test-bed experiment, and the reliability of the threshing device was verified through field experiments.

2   Materials and methods

2.1   Structure of threshing device

The threshing device including screw feeder, threshing rasp bar, separating rod, impurity removing rod, and so on[16], as shown in Figure 1. The working process of threshing device can be divided into feeding, threshing, impurity removal. The rotating direction of threshing cylinder is clockwise from the direction of feeder, which is consistent with the installation direction of feeder guide plate to ensure smooth feeding of wheat ears into threshing chamber. When threshing rasp rod rotates at high speed, it impacts and rubs against the ears, thus removing maize kernels from ears. Subsequently, the core shaft segment that has not been removed moves along with the rotation of threshing cylinder to separate the nail tooth segment, completely separating the particles from core shaft, and finally discharged out of the device under the action of the impurity removing rod.
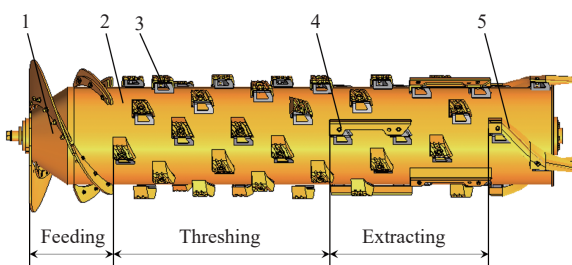
1-Rotational axis 2-Screw feeder 3-Threshing rasp bar 4-Separating rod 5-Impurity removing rod.

Figure 1   Diagram of maize threshing device

Compared with the existing threshing cylinders[5-7], most of them with a single form were weak in handling maize ears, however, the device designed in this study adopted rasp bar type thresher, which has a larger interaction area with maize ears than the nail tooth, and more damage on maize kernels was avoided. The

use of separating rod can better separate the maize kernels from broken mandrels and other impurities, and get cleaner maize kernels. The impurity removing rod can accelerate the discharge of miscellaneous slag, improve the feeding capacity of the threshing device and prevent the threshing cylinder from blocking.

2.2   Analysis of "Kernel-kernel" contact model and "Kernel-mechanical" interaction system

DEM is a common method for kinematic analysis of granular materials[17,18], and it is increasingly used to simulate the mechanical production process of agricultural crops[8,19,20]. EDEM is a discrete element software developed by DEM-solution Company, which provides a solution for the movement, power, heat, and energy transfer of particle flow, and reduces the development cost and time. EDEM regards the research object as discrete and independent moving particles, establishes the motion equation of each particle according to Newton's second law, and solves the motion parameters by using the display center difference method. The deformation and evolution of the object are represented by the relative motion of discrete particles. Besides boundary conditions, the constitutive equation, equilibrium equation, and deformation compatibility equation need to be satisfied when solving the problems of continuum mechanics. EDEM uses the circular calculation method to track and calculate the movement of particles. The basic flow chart was shown in Figure 2.
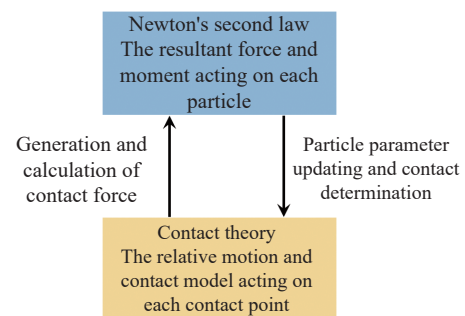
Figure 2   EDEM internal calculation relationship

Considering that maize kernel is a viscoelastic biomaterial, soft ball model should be chosen as a simplified model[21,22], the simplified treatment of the contact force between particles in the soft ball model was shown in Figure 3[23]. The contact normal force F_{nij} between particles is the total force of elastic force and damping force exerted by spring and normal damper on the particles. According to Hertz contact theory, the contact normal force F_{nij} and contact tangential force $F_{\tau ij}$ are expressed by Equation (1).

$$\begin{cases} F_{nij} = \left(-k_n\lambda^{\frac{3}{2}} - c_n v_{ij} \cdot n\right) n \\ F_{\tau ij} = -k_\tau\delta - c_\tau v_{ct} \end{cases} \tag{1}$$

where, δ and λ are the normal overlap and tangential overlap, respectively; k_n and k_τ is the normal elastic coefficient and tangential elastic coefficient of kernel, respectively; c_n and c_τ is the normal damping coefficient and tangential damping coefficient of kernel, respectively; v_{ij} is velocity of particle i to particle j; n is unit vector from the spherical center of particle i to the spherical center of particle j; v_{ct} is sliding speed of contact point, as expressed by Equation (2).

$$v_{ct} = v_{ij} - \left(v_{ij} \cdot n\right) n + R_i\omega_i \times n + R_j\omega_j \times n \tag{2}$$

where, R_i and R_j are the radius of kernel i and kernel j, respectively; ω_i and ω_j are the angular velocity of kernel i and kernel j, respectively. When $|F_{\tau ij}|>\mu s|F_{nij}|$, the kernel will slip.

The static motion equation of ear during threshing process is shown as Equation (6).

$$\begin{cases} f_1 \sin\alpha + F\cos\beta + G = N\cos\alpha + f_2\sin\beta \\ N\cos\alpha + f_1\sin\alpha = F\sin\beta + f_2\cos\beta \end{cases} \quad (6)$$

Equation (7) is obtained through Equation (6).

$$\begin{cases} N(\mu_1\sin\alpha - \cos\alpha) + G = F(\mu_2\sin\beta - \cos\beta) \\ N(\cos\alpha + \mu_1\sin\alpha) = F(\sin\beta + \mu_2\cos\beta) \end{cases} \quad (7)$$

Finally, the force F of thresher on whole ear is shown in Equation (8), and when force F is greater than the right side of equal sign, the ear starts to move.

$$F = G\frac{\cos\alpha + \mu_1\sin\alpha}{(\sin\beta + \cos\beta)(\mu_1\sin\alpha - \mu_2\cos\alpha) + \cos\alpha(\cos\beta - \sin\beta)} \quad (8)$$

where, μ_1 is friction coefficient of concave; μ_2 is friction coefficient of thresher.

Assuming that the particle acting force is constant in the calculation time distance during the kernel movement, the Euler expression of the particle movement equation obtained according to Newton's second law is shown in Equation (9).

$$\begin{cases} F_\xi(t) + mg_\xi - \beta_g v_\xi(t) = m\dfrac{dv_\xi}{dt} \\ M_\xi(t) - \beta_g \omega_\xi(t) = I\dfrac{d\omega_\xi}{dt} \end{cases} \quad (9)$$

where, ξ is components in axis x, y, and z of space, respectively; $F_\xi(t)$ is the total force of kernel at time t, N; g_ξ is components of gravity in axis x, y, and z; β_g is the global damping coefficient, and the artificial damping added in the dynamic relaxation method; $v_\xi(t)$ is average velocity component of kernel at time t, m/s; M_ξ is the total moment produced by the contact force, N·m; $\omega_\xi(t)$ is the rotation speed of kernel at time t, r/min; I is the rotational inertia of kernel, kg·m².

Equation (9) can be rewritten as Equation (10).

$$\begin{cases} F_\xi(t) + mg_\xi - \beta_g\dfrac{v_\xi(t) - v_\xi(t-\Delta t)}{2} = m\dfrac{v_\xi(t) - v_\xi(t-\Delta t)}{dt} \\ M_\xi(t) - \beta_g\dfrac{\omega_\xi(t) - \omega_\xi(t-\Delta t)}{2} = I\dfrac{\omega_\xi(t) - \omega_\xi(t-\Delta t)}{dt} \end{cases} \quad (10)$$

According to Equation (10), the kernel velocity and angular velocity can be calculated by Equation (11).

$$\begin{cases} v_\xi(t) = v_\xi(t-\Delta t)\dfrac{m/\Delta t - \beta_g/2}{m/\Delta t + \beta_g/2} + \dfrac{F_\xi(t) + mg_\xi}{m/\Delta t + \beta_g/2} \\ \omega_\xi(t) = \omega_\xi(t-\Delta t)\dfrac{I/\Delta t - \beta_g/2}{I/\Delta t + \beta_g/2} + \dfrac{M_\xi(t)}{m/\Delta t + \beta_g/2} \end{cases} \quad (11)$$

Then, the average displacement $u(t)$ and rotational displacement $\theta(t)$ are shown in Equation (12).

$$\begin{cases} u(t) = u(t-\Delta t) + v_\xi(t)\Delta t \\ \theta(t) = \theta(t-\Delta t) + \omega_\xi(t)\Delta t \end{cases} \quad (12)$$

According to Equations (6)-(12), the force of thresher on maize kernels is closely related to its moving velocity and other parameters. As known from theoretical analysis results, the bigger the force generated by thresher, the higher the moving velocity of maize kernels, and the easier it is to damage the maize kernels during threshing. Therefore, it is of great significance to study the structure and working parameters of thresher to reduce maize kernel broken rate.

2.3　Simulation experiment conditions

In practical research, the parameters can be controlled such as

a. Normal force　　　　　b. Tangential force

c. Diagram of ear static analysis

Note: ω is angular velocity and direction of threshing cylinder, r/min; N is force of concave on ear, N; F is force of threshing cylinder on ear, N; G is gravity of ear, N; M is total torque of ear, N·m; f_1 is friction between concave and ear, N; f_2 is friction between thresher and ear, N; α is angle between force N and vertical direction, (°); β is angle between force F and vertical direction, (°).

Figure 3　Diagram of particle contact force in soft ball model simplified processing

The total force and moment of the particles are as Equation (3).

$$\begin{cases} \boldsymbol{F}_{ij} = \boldsymbol{F}_{nij} + \boldsymbol{F}_{\tau ij} \\ \boldsymbol{T}_{ij} = R_i \boldsymbol{n} \times \boldsymbol{F}_{\tau ij} \end{cases} \quad (3)$$

When there are multiple kernels, kernel i is in contact with multiple kernels at the same time, and the total force F_i and moment acting M_i on kernel i are shown in Equation (4).

$$\begin{cases} F_i = \sum_j \left(F_{nij} + F_{\tau ij} \right) \\ M_i = \sum_j \left(R_i n \times F_{\tau ij} \right) \end{cases} \quad (4)$$

In the soft ball model, the elastic coefficient and damping coefficient are related to the elastic modulus and Poisson's ratio of kernel, and the normal elastic coefficient, damping coefficient, tangential elastic coefficient and damping coefficient of kernel are shown in Equation 5.

$$\begin{cases} k_n = \dfrac{4}{3}\left(\dfrac{1-\upsilon_i^2}{E_i} + \dfrac{1-\upsilon_j^2}{E_j}\right)^{-1}\left(\dfrac{R_i+R_j}{R_iR_j}\right)^{-\frac{1}{2}} \\ c_n = 2\sqrt{mk_n} \\ k_t = 8\sqrt{\delta}\left(\dfrac{1-\upsilon_i^2}{G_i} + \dfrac{1-\upsilon_j^2}{G_j}\right)^{-1}\left(\dfrac{R_i+R_j}{R_iR_j}\right)^{-\frac{1}{2}} \\ c_\tau = 2\sqrt{mk_\tau} \end{cases} \quad (5)$$

where, υ_i and υ_j are Poisson's ratio of kernel i and j; E_i and E_j are the elastic modulus of kernel i and j, MPa; R_i and R_j are the radius of kernel i and j; G_i and G_j are shear modulus of kernel i and j, MPa; m is mass of kernel, kg.

threshing cylinder speed, concave clearance, and feeding amount by visual and manual methods. However, removing the threshing rasp bars will lead to the deterioration of threshing cylinder dynamic balance during operation, in addition, manufacturing threshers with different structures and materials require an extremely complicated manufacturing process, which increases the research cost and time. Therefore, for the parameters such as installation distance and material properties of threshing rasp bars, which are difficult to be observed through ordinary methods, the simulation experiments were carried out to study them in this study. The structural parameters of threshing device were determined through simulation experiment, which also provides a new idea for the design of production equipment for other crops.

The simulation experiments were run in EDEM 2018 (Engineering discrete element method, DEM Solution Ltd.) environment, EDEM simulation operation steps were as follows: 1) Combined with previous biomechanical parameter tests and references, thresher materials, and maize materials were established. Considering the influence of threshing cylinder materials on threshing effect, the materials of threshing cylinder were rubber, cast iron, and 50Mn steel[24]; 2) Mechanical parameters between kernel and threshing cylinder were set, such as sliding friction coefficient and collision recovery coefficient, as listed in Table 1 and 2[3,25-29]; 3) Added to three interaction models that "Particle to Particle", "Particle to Geometry", and "Particle Body Force", there was basically no adhesion on kernel surface, so the Hertz-Mindlin no slip model was selected for "Particle to Geometry", and the discrete element model of kernel was generated by particle filling method, so the Hertz-Mindlin with bonding model was selected for "Particle to Particle". The Particle Body Force selected the complied file of particlereplacement.dll to define the replacement parameters of kernels; 4) In addition to the rotation of threshing cylinder, a particle factory was added at the installation connection point of cylinder screw feeder. In the actual harvest, 45 kernels were generated according to the feeding amount of 10 kg/s, with random direction and position; 5) The time step was 20% of Rayleigh time, the total simulation time was set to 5 s, the calculation interval was 0.01 s, the minimum calculation radius was twice the particle radius, and 9 040 896 units were generated in total. The purpose of simulation experiment was to obtain the influence of various factors coupling on threshing effect, the parameters of single factor test are listed in Table 3.

Table 1   Contact parameter setting

Contact type	Kernel-kernel	Kernel-rubber	Kernel-cast iron	Kernel-50Mn steel
Restitution coefficient	0.25	0.56	0.90	0.60
Coefficient of static friction	0.09	0.35	0.22	0.30
Coefficient of rolling friction	0.01	0.03	0.01	0.01

Table 2   Material properties

Parameters	Kernel	Rubber	Cast iron	50Mn steel
Poisson's ratio	0.4	1.35	6.9	7.85
Shear modulus/MPa	1.37×10^2	0.47	0.25	0.35
Density/(g·cm⁻³)	1.197	7.84	4.5×10^4	7.9×10^4

Table 3   Single factor test levels

Parameter	Unit	Values
Threshing cylinder speed	r/min	300, 350, 400
Installation distance of threshers	mm	200, 250, 300
Materials of threshing device		Rubber, cast iron, 50Mn steel

3   Results and discussion

3.1   Influence of installation distance of threshing rasp bar

In practice, frequent disassembly of threshers will adversely affect the dynamic balance of threshing cylinder, and there is a potential safety hazard during the experiments, therefore, the simulation experiments can effectively avoid this problem. In this simulation experiment, the threshing cylinder speed was set as 350 r/min. The total force of kernels of the simulation test was shown in Figure 4a, maize ear threshing was achieved by the force generated by the "crop-mechanical" interaction system. According to the law of conservation of energy, after the maize ears entered the threshing device, they were impacted and rubbed by threshers and concave, and the energy obtained by maize core was greater than the inherent energy of its own organizational structure, so the structure of maize core was further damaged and finally broken. Subsequently, under the mutual extrusion and collision between the maize ears, the threshing was completed.
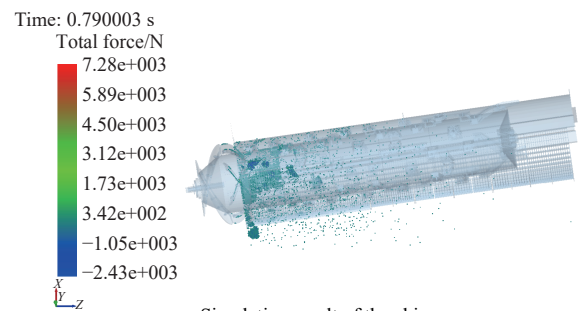
a. Simulation result of threshing process
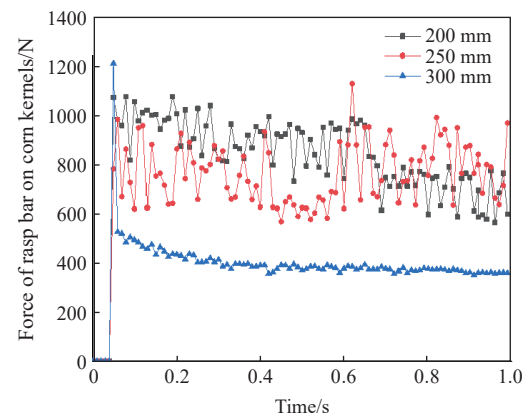
b. Normal force of threshers acted on ears
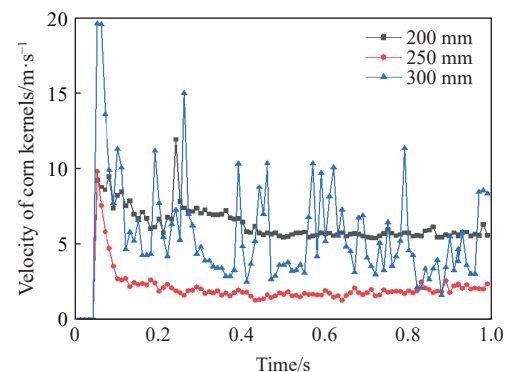
c. Average velocity of kernels in threshing device

Figure 4   Simulation results of threshing process and contact force of threshers on ears

The forces of thresher on maize kernels are shown in Figure 4b, while the velocities of maize kernels in threshing device are shown

in Figure 4c. Under the coupling effect of installation distance and threshing cylinder speed, the forces exerted by threshers on ears presented different trends. Generally, the speed change of threshing cylinder has a more significant impact on threshing effect, because the higher the speed, the higher the kinetic energy of threshing cylinder and the greater the energy acting on ears, which is directly related to the kernel movement speed. The force and velocity of maize kernels were two indexes to reflect the threshing effect of maize ears and predict whether the maize kernel may be damaged by secondary impact. When the installation distance of rasp bar was set as 200 mm, the average force acted on maize kernels was 803.07 N, while the average velocity of maize kernels was 6.02 m/s. When it was set to 250 mm, the average force and velocity of maize kernels were 727.13 N and 2.08 m/s, respectively. When it was set at 300 mm, the average force and velocity of maize kernels were 383 N and 5.51 m/s, respectively. The simulation results showed that there was a non-linear relationship between the force of maize kernels and the installation distance of rasp bar. Although the force of the maize kernels was the smallest when the installation distance was 300 mm, the moving velocity was the highest. Correspondingly, the force of maize kernels was the biggest when the installation distance was 200 mm. According to the change curves of force acted on maize kernels and velocity of maize kernels in the whole simulation process, when the, the value of force and velocity of maize kernels were always at a high level under the situation of thresher installation distance was 200 mm, this was because the rasp bars were arranged too densely, maize ears were easily impacted by frequent impact forces from threshers to accelerate threshing, but the maize kernels after threshing may move too fast to impact other threshers again and be damaged. According to research results reported by Chandio et al.[30], the range of vertical rupture force of maize kernel was 180-328.2 N, while the lateral force was 524-715 N, which were basically consistent with the simulation results. The force value of maize kernels fluctuated greatly when the installation distance is 250 mm, which indicated that the maize ears were constantly in full contact with the rasp bars for threshing, and the maize kernels moving velocity after threshing were at a low level, which denoted that the maize kernels were basically completely separated from the maize ears, and only continued to move inertia under the action of gravity, without secondary contact with other threshers, which can effectively avoid the damage of maize kernels. With the increased installation distance of threshers, the force acted on maize kernel decreased, the arrangement of threshers was too sparse, and the contact frequency between maize ears and rasp bars was poor, so it was impossible to thresh sufficiently. And the maize ears moved with the threshing cylinder rotating, which led to a large fluctuation in the velocity of maize kernels, it was not conducive to maize ears threshing. Combined with the above analysis, the installation distance of rasp bars with 250 mm was a ideal structure parameter.

3.2 Influence of threshing cylinder speed

The research showed that the threshing cylinder speed has a significant influence on kernel broken rate[16,31]. When the installation distance of threshers was set as 250 mm, the changing laws of force and velocity of maize kernels under different threshing cylinder speed were shown in Figures 5a and 5b respectively. With the increased of threshing cylinder speed, the force of threshers increased overall. As the threshing cylinder speed was 300 r/min, the average force of maize kernels was 235.65 N, while the average velocity of maize kernels was 4.67 m/s. Similarly, as the threshing cylinder speed was 350 r/min, the force of maize

kernels was the smallest and the fluctuation difference was small, with an average value of 201.7 N, a maximum value of 342.0 N, and a minimum value of 104.3 N, while the maximum value of maize kernel velocity was 21.7 m/s, the minimum was 1.62 m/s, and the average velocity was 5.49 m/s. As the speed increased at 400 r/min, the maximum normal force exceeded 2×10^3 N, the maximum velocity of kernels was 10.46 m/s, the minimum velocity was 7.84 m/s, and the average velocity was 22.52 m/s. Obviously, it far exceeded the maximum destructive power of maize kernel, and the numerical value fluctuated violently, which indicated that the maize kernels were constantly in contact with the threshers at a higher rotating speed of threshing cylinder. The experimental experience showed that the higher the threshing cylinder speed, the higher the threshing efficiency, which meant that it was likely to cause greater damage to maize kernels.
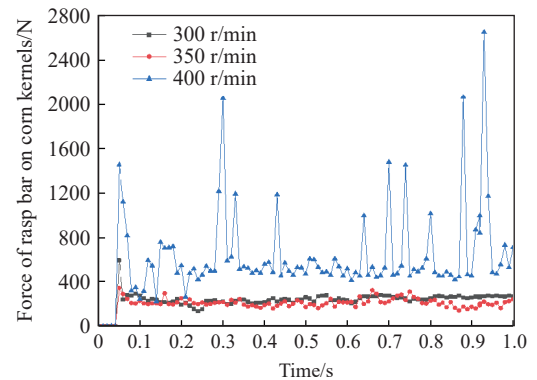
a. Force of thresher acted on kernels
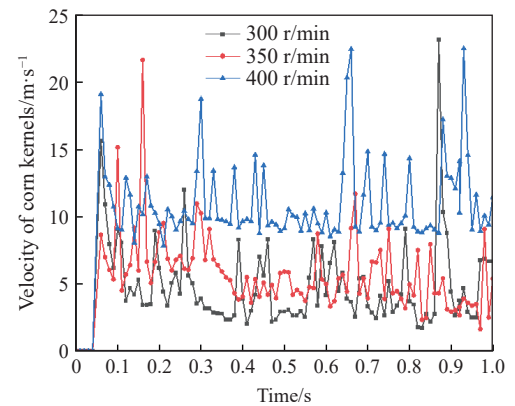
b. Velocity of kernels in threshing device

Figure 5　Influence of normal force on kernels

Therefore, choosing the proper speed of threshing cylinder cannot only meet requirements of threshing efficiency, but also ensure the minimum kernel damage. With the speed of threshing speed increasing, it would not only be impacted by thresher under the condition of high rotating speed, but also continue to accelerate under the action of inertia force, the phenomenon of kernel damage may also occur in this process. According to the simulation results, it was more beneficial to ears threshing with the speed of threshing cylinder was 300 r/min or 350 r/min, the force curve and velocity curve of maize kernels did not fluctuate violently, and it was no significant difference in the effect of threshing rasp bars on maize ears, so the parameter of threshing cylinder speed needed to be further verified by test-bed experiments.

3.3 Influence of material properties of threshing rasp bar

For studying the influence of thresher material properties on threshing effect, due to the thresher dies made of different materials

have long production cycle and labor cost, changing the material properties of threshing device models with in simulation environment can effectively improve the research and development efficiency, and calculate more accurate results. Therefore, three kinds of materials were adopted for threshers, the parameters and contact properties with maize kernels are listed in Table 1 and Table 2, respectively.

The simulation results of force and velocity of maize kernels were shown in Figure 6. When rubber material was adopted for thresher, there was flexible contact between maize kernels and rasp bars, the maximum force of maize kernels was 329.22 N, the minimum value was 156 N, and the average value was 63.44 N. As known from Figure 6c, obviously, this material had the least damage to maize kernels, but the adhesion between threshers and maize ears was very strong, so as to the maize kernels cannot be threshed sufficiently under insufficient force. Considering the influence of friction, impact, and decay in practical work, rubber material is easy to wear and has short service life, in addition, frequent replacement of materials will adversely affect the stability of threshing devices. Therefore, rubber material is not the most ideal material for maize ear threshing. When case iron material was

a. Force of threshers acted on kernel

b. Velocity of kernels in threshing device

c. Simulation results with rubber materials

Figure 6   Influence of materials of threshers on force and velocity

used for product thresher, the minimum value of force acted on kernels was 1506 N, and the average value was 2254 N; when the 50Mn steel was utilized, the minimum force was 674 N, and the average force was 1343 N. In practice, compared with cast iron material and 50Mn steel material, cast iron material is easy to cause great damage to kernels. Combined with the above analysis, the material of thresher was chosen 50Mn steel.

3.4   Test-bed experiment results

According to the simulation experiment results, it was found that the installation distance on threshing cylinder and the material of threshing rasp bar was 250 mm and used 50Mn steel, which were the ideal parameters. In order to further determine the working parameters of threshing device, a maize threshing test-bed was set up for experimental study. As shown in Figure 7, the test-bed comprised a feeding device, threshing device, cleaning device, power drive system, and frame, wherein the cleaning device comprised a rocking plate, upper sieve, lower sieve, tail sieve, and crank mechanism. During experiment, according to accumulation of previous test data, the speed of fan and vibrating screen in cleaning device was 900 r/min and 265 r/min. On the basis of the actual harvest situation, the ear feeding amount was converted into 6 kg/s, 8 kg/s, and 10 kg/s respectively, and the concave clearance was converted into 35 mm, 40 mm, and 45 mm. The experiments were conducted according to "GB/T 21962-2020 Maize combine harvesters". After the test, no less than 2 kg of kernels were collected at kernel collecting port, 500 g of kernels were randomly selected and weighed three times, and the kernels with skin injuries and eating meat were selected and weighed, the kernel broken rate was calculated, and the average value was taken as the final result. Each group of experiments was repeated three times, and the regression analysis is shown in Figure 8. Table 4 lists the orthogonal experiment scheme and results, it was designed in Design Expert software, with the maize kernel broken rate as the evaluation index, and ANOVA results are listed in Table 5.
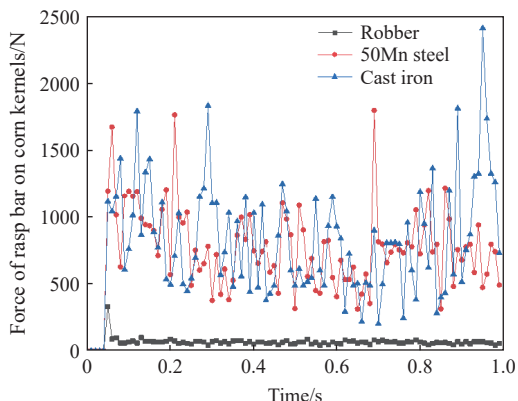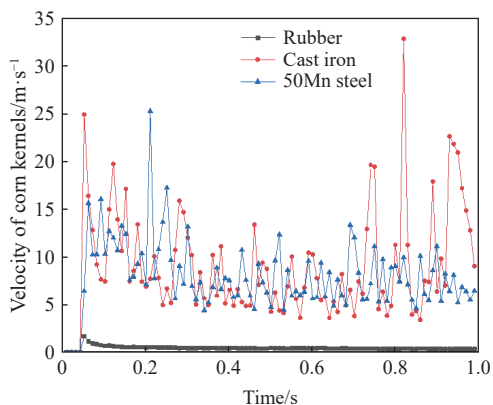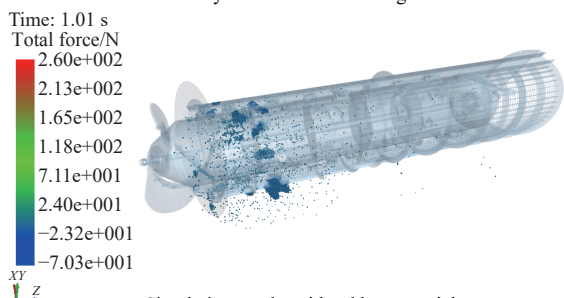
1. Maize feeding device 2. Threshing device 3. Cleaning device 4. Frame 5. Power-driven system

Figure 7   Test bed of maize threshing.

According to the analysis of orthogonal experiment results, it showed that the effect of threshing cylinder speed, concave clearance, and feeding amount on the kernel broken rate have extremely significant, the order of influence degree was as follows: $A>B>C$. There was interaction among the above three factors, $0.01 <$ Prof. $AB<0.05$ showed that interaction of threshing cylinder speed and concave clearance was obvious, while Prof. $AC>0.01$ and Prof. $BC>0.01$ showed that the interaction of threshing cylinder speed combined with feed amount and concave clearance combined with feed amount was extremely obvious. According to test results, the

a. Influence of threshing cylinder speed and concave clearance on kernel broken rate

b. Influence of threshing cylinder speed and feed amount on kernel broken rate

c. Influence of concave clearance and feed amount on kernel broken rate
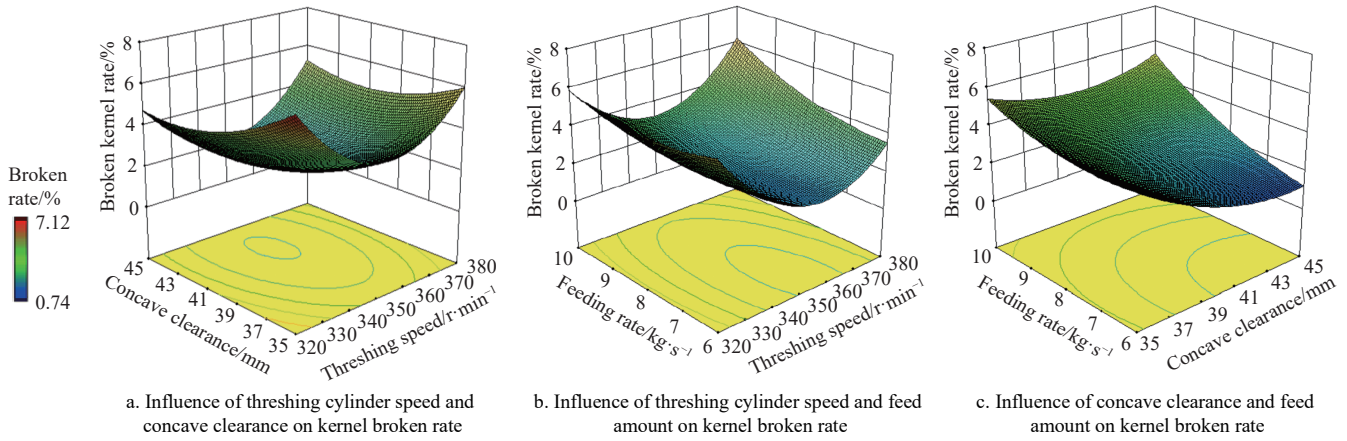
Figure 8   Response surface analysis of orthogonal test results

Table 4   Orthogonal test scheme and results

No.	A-Threshing cylinder speed/r·min^{-1}	B-Concave clearance/mm	C-Feeding amount/kg·s^{-1}	Kernel broken rate/%
1	350	40	8	1.78
2	350	35	6	4.08
3	320	40	6	5.07
4	380	40	6	2.88
5	320	35	8	7.12
6	350	40	8	1.56
7	380	40	10	6.32
8	320	40	10	5.86
9	320	45	8	4.20
10	350	40	8	1.62
11	350	45	6	0.74
12	350	40	8	1.88
13	350	45	10	3.65
14	350	40	8	1.34
15	380	45	8	4.29
16	350	35	10	4.08
17	380	35	8	5.74

Table 5   ANOVA of kernel broken rate

Source	Sum of squares	df	Mean square	F-value	p-value (Prob>F)
Model	60.57	9	6.73	102.21	<0.0001
A-Threshing cylinder speed	33.98	1	33.98	516.09	<0.0001
B-Concave clearance	5.19	1	5.19	78.86	<0.0001
C-Feed amount	4.66	1	4.66	70.70	<0.0001
AB	0.54	1	0.54	8.20	0.0242
AC	1.76	1	1.76	26.66	0.0013
BC	2.12	1	2.12	32.15	0.0008
A^2	32.97	1	32.97	500.70	<0.0001
B^2	3.44	1	3.44	52.17	0.0002
C^2	1.51	1	1.51	22.89	0.0020
Residual	0.46	7	0.066		
Lack of Fit	0.29	3	0.096	2.20	0.2306
Pure Error	0.17	4	0.043		
Cor Total	61.03	16			
Model	60.57	9	6.73	102.21	<0.0001

response surface fitting results of the factors affecting kernel broken rate are obtained, as shown in Figure 2. The denser the circular arcs on the projection plane, the more remarkable the effect, the more significant the effect was. Removing the parameters that have no

effect on evaluation index, the quadratic regression prediction equation of kernel broken rate can be obtained as shown in Equation (13).

The regression equation calculated from actual data can predict the operation quality of the test-bed. Because the coefficients involved in Equation (13) are scaled to suit the unit of each factor, and the intercept was not in the center of the design space, they are not used to determine the influence of each factor.

$$R_G = 547.36 - 2.38A - 4.53B - 8.72C + 0.002\,45AB + 0.011AC + 0.073BC + 0.0032A^2 + 0.036B^2 + 0.15C^2 \quad (13)$$

As shown in Figure 8a, the effect of concave clearance and threshing cylinder speed on kernel broken rate when maize ear feeding amount was 8.74 kg/s. With the increase of concave clearance and threshing cylinder speed, kernel broken rate first decreased and then increased. The main reason was that ears stayed in threshing device for a long time with small concave clearance and low threshing cylinder speed, causing mutual extrusion and collision force was large. When threshing cylinder speed was high, the impact force of thresher on ear increased, and kernels were easily damaged during threshing. As shown in Figure 8b, when concave clearance was 38.6 mm, with increasing threshing cylinder speed, the kernel broken rate still decreased at first and then increased. The kernel broken rate was the lowest when threshing cylinder speed was 350 r/min. And ears were threshed more fully with feed amount increased but its broken rate also increased. As shown in Figure 8c, when threshing cylinder speed was 369 r/min, the kernel broken rate decreased gradually with the increase of concave clearance and decreasing of feed amount. It was because the movement space of ears in threshing device became large, and the interaction of impact and collision of ear-concave and ear-threshers were smaller. Besides, the contact friction between ears was insufficient to separate maize kernels from mandrel leading to inadequate threshing operation. In Design Expert, kernel broken rate was taken as optimization target, the kernel broken rate was smaller than 2% as optimization requirements. The result as shown in Figure 9 indicated that the optimal working parameters were threshing cylinder speed 356 r/min, concave clearance 40 mm, and feed amount 8 kg/s, at this time, the kernel broken rate was 1.65%. Compared with the results reported by other research institutions[3,5,6,32], the threshing device designed in this study has the lowest kernel broken rate, but the working parameters of threshing devices were different, which was caused by different experiment environments and maize varieties.

320   380   35   45   6   10

A: Threshing cylinder speed=356.296   B: Concave clearance=40.8889   C: Feeding amount=8.18272

0   2   Desirability=1.000

0.74   7.12

Grain broken rate=1.65245
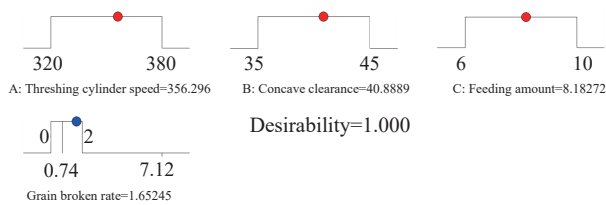
Figure 9   Results of optimization parameters

3.5   Field experiment results

According to the optimization parameters of test-bed experiment results, the field experiment was carried out to verified the simulation experiment results and the test-bed experiment results. This experiment was conducted in Qingdao City, Shandong Province of China. According to "NY/T 1355-2007 Maize Harvesters-Operating Quality" and "GB/T 21962-2020 Maize Combine Harvester". The length of the experiment site was 40 m, including preparation area of 10 m, survey area of 20 m, and parking area of 10 m. At the end of the experiment, less than 2000 g of maize kernels were taken out from the granary, and about 500 g of kernels samples were randomly taken out by the five-point sampling method. The broken maize kernels were selected and weighed. The calculation method of grain breakage rate is shown in Equation (14). In this experiment, the control accuracy of maize harvester cannot reach the decimal point order, thus the threshing cylinder speed was about 356 r/min, the concave clearance was 40 mm, and the feeding amount was 8 kg/s. The experiment was

repeated for 3 times, and the average value of kernel broken rate was calculated, the results are listed in Table 6. Figure 10 showed the field experiment, and the threshing performance of threshing device is shown in Figure 11, it shows the process of selecting broken kernels, the results of weighing the broken grains, and the complete kernels lost in the field, respectively. In summary, the direct kernel harvester has a deal threshing performance.

Table 6   Field experiment results

No.	Kernel broken rate/%	Average/%	Standard deviation
1	1.88		
2	2.06	1.93	0.07
3	1.95		

Figure 10   Field experiment

a. Selecting broken kernels form the sample   b. Broken kernels weighing   c. Complete kernels lost in the field
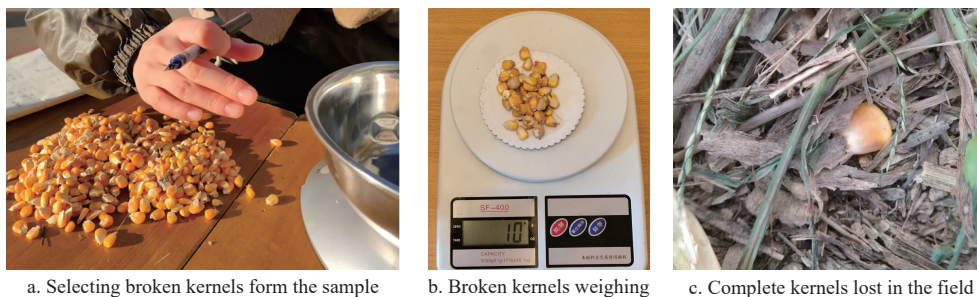
Figure 11   Threshing effect

$$R = \frac{1}{5}\sum_{i=1}^{5}\frac{m_i}{m_{si}} \times 100\% \qquad (14)$$

where, m_i is the mass of broken kernels, g; m_{si} is the mass of maize kernels sample, g.

The kernel broken rate was 1.93% in field working conditions, which was 0.28% higher than the optimization results, it is because that the working environment in the field is more complicated and changeable. The external factors such as soil conditions, weather, other operation parameters of harvesting machinery, machine vibration will directly affect the harvesting performance, but this difference was still within the allowable range, and the kernel broken rate met the standard requirements.

4   Conclusions

In view of the problem of lack of accurate and efficient research technology in the design optimization of maize threshing device, this study determined the structure parameters of rasp bar based on discrete element method, and obtained the influence of threshing rasp bar on maize kernels. It is verified that simulation technology can eliminate the technical obstacles in the optimal design of maize ear threshing device, which provides reference for other crop production technologies. The main conclusions were as

follows.

1) The maize kernel was simplified as soft ball model based on discrete element method, the interaction viscoelastic model of "crop-machinery" was constructed, and the mechanical parameters such as force, velocity, torque, and deformation of normal contact and tangential contact between kernel and thresher was analyzed, to obtain the main factors affecting the ear kinematics, including the characteristics of maize physical and mechanical characteristics, the material properties of thresher, the speed of threshing cylinder and other working parameters.

2) In order to solve the problem that structural parameters of threshing device was difficult to design, the simulation experiment was utilized to select the structural parameters of threshing device. The threshing cylinder speed, installation distance, and material characteristics of rasp bar were simulated. Through the analysis of force and velocity of maize kernels, this study expounded the threshing mechanism of maize ears, and obtained the influence of threshing device structure and working parameters on threshing effect. The simulation experiment results showed that the threshing device has better working performance when installation distance of threshing rasp bars was 250 mm, made of 50Mn steel, and the threshing cylinder speed was 350 r/min;

3) The working parameters of threshing device were further determined through test-bed experiment, and the optimal combination obtained by orthogonal analysis optimization results was as follows: threshing cylinder speed was 356 r/min, concave clearance was 40 mm and feeding amount was 8 kg/s. Finally, the field experiment verified the kernel broken rate was 1.93%, which met the standard requirements.

Acknowledgements

[References]

[1] Cui T, Fan C L, Zhang D X, Yang L, Li Y B, Zhao H H. Research progress of maize mechanized harvesting technology. Transactions of the CSAE, 2019; 50(12): 1–13. (in Chinese)

[2] Su Z, Li Y M, Dong Y H, Tang Z, Liang Z W. Simulation of rice threshing performance with concentric and non-concentric threshing gaps. Biosystems Engineering, 2020; 197: 270–284.

[3] Chen M Z, Xu G F, Wang C X, Diao P S, Zhang Y P, Niu G D. Design and experiment of roller-type combined longitudinal axial flow flexible threshing and separating device for corn. Transactions of the CSAE, 2020; 51(10): 123–131. (in Chinese)

[4] Powar R V, Aware V V, Shahare P U. Optimizing operational parameters of finger millet threshing drum using RSM. Journal of Food Science and Technology, 2019; 56: 3481–3491.

[5] Wang Z D, Cui T, Zhang D X, Yang L, He X T, Zhang Z P. Design and experiment of low damage corn threshing drum with gradually changing diameter. Transactions of the CSAE, 2021; 52(8): 98–105. (in Chinese)

[6] Fan C L, Cui T, Zhang D X, Yang L, Qu Z, Li Y H. Design and test of low-damage combined corn threshing and separating device. Transactions of the CSAE, 2019; 50(4): 113–123. (in Chinese)

[7] Yu Y J, Li L S, Zhao J L, Wang X G, Fu J. Optimal design and simulation analysis of spike tooth threshing component based on DEM. Processes, 2021; 9(7): 1163.

[8] Cundall P A, Strack O D L. A discrete numerical model for granular assemblies. Geotechnique, 1979; 29(1): 47–65.

[9] Chai X Y, Zhou Y, Xu L Z, Li Y, Li Y M, Lyu L Y. Effect of guide strips on the distribution of threshed outputs and cleaning losses for a tangential-longitudinal flow rice combine harvester. Biosystems Engineering, 2020; 198: 223–234.

[10] Binelo M O, Lima R F, Khatchatourian O A, Stransky J. Modelling of the drag force of agricultural seeds applied to the discrete element method. Biosystems Engineering, 2019; 178: 168–175.

[11] Shi Y Y, Xin S, Wang X C, Hu Z C, Newman D, Ding W M. Numerical simulation and field tests of minimum-tillage planter with straw smashing and strip laying based on EDEM software. Computers and Electronics in Agriculture, 2019; 166: 105021.

[12] Liang Z W, Li Y M, Baerdemaeker J D, Xu L Z, Saeys W. Development and testing of a multi-duct cleaning device for tangential-longitudinal flow rice combine harvesters. Biosystems Engineering, 2019; 182: 95–106.

[13] Xu L Z, Wei C C, Liang Z W, Chai X Y. Development of rapeseed cleaning loss monitoring system and experiments in a combine harvester. Biosystems Engineering, 2019; 178: 118–130.

[14] Ma X D, Guo B J, Li L L. Simulation and experiment study on segregation mechanism of rice from straws under horizontal vibration. Biosystems Engineering, 2019; 186: 1–13.

[15] Yu Y J, Fu H, Yu J Q. DEM-based simulation of the corn threshing process. Advanced Powder Technology, 2015; 26(5): 1400–1409.

[16] Li X Y, Du Y F, Guo J L, Mao E R. Design, simulation, and test of a new threshing cylinder for high moisture content corn. Applied Sciences, 2020; 10(14): 4925.

[17] Olsson E, Jelagin D. A contact model for the normal force between viscoelastic particles in discrete element simulations. Powder Technology, 2019; 342(15): 985–991.

[18] Horabik J, Wiacek J, Parafiniuk P, Stasiak M, Banda M, Molenda M. Tensile strength of pressure-agglomerated potato starch determined via diametral compression test: Discrete element method simulations and experiments. Biosystems Engineering, 2019; 183: 95–109.

[19] Sun H Y, Ma H Q, Zhao Y Z. DEM investigation on conveying of non-spherical particles in a screw conveyor. Particuology, 2022; 65: 17–31.

[20] Zeng Z W, Chen Y, Qi L. Simulation of cotyledon-soil dynamics using the discrete element method (DEM). Computers and Electronics in Agriculture, 2020; 174: 105505.

[21] Shmulevich I. State of the art modeling of soil–tillage interaction using discrete element method. Soil and Tillage Research, 2010; 111(1): 41–53.

[22] Zhou Y H. A theoretical model of collision between soft-spheres with Hertz elastic loading and nonlinear plastic unloading. Theoretical and Applied Mechanics Letters, 2011; 1(4): 041006.

[23] Horabik J, Molenda M. Parameters and contact models for DEM simulations of agricultural granular materials: A review. Biosystems Engineering, 2016; 147: 206–225.

[24] Gao X J, Cui T, Zhou Z Y, Yu Y B, Xu Y, Zhang D X, et al. DEM study of particle motion in novel high-speed seed metering device. Advanced Powder Technology, 2021; 32(5): 1438–1449.

[25] Wang X M, Yu J Q, Lv F Y, Wang Y, Fu H. A multi-sphere based modelling method for maize grain assemblies. Advanced Powder Technology, 2017; 28: 584–595.

[26] Moysey P A, Thompson M R. Determining the collision properties of semi-crystalline and amorphous thermoplastics for DEM simulations of solids transport in an extruder. Chemical Engineering Science, 2017; 62(14): 3699–3709.

[27] Chung Y Y, Jeong Y W, Park Y L, Kim J J, Moon J S, Fu J, et al. Postnatal Development of brain natriuretic peptide-immunoreactive neuron in the hypothalamus of the rat, Korean J. Phys. Anthropol, 2004; 17(1): 1–10.

[28] Gonzáalez-Montellano C, Fuentes J M, Ayuga-Tèllez E, Ayuga F. Determination of the mechanical properties of maize grains and olives required for use in DEM simulations. Journal of Food Engineering, 2012; 111(4): 553–562.

[29] Markauskas D, Ramírez-Gómez Á, Kačianauskas R, Zdancevičius E. Maize grain shape approaches for DEM modeling. Computers and Electronics in Agriculture, 2015; 118: 247–258.

[30] Chandio F A, Li Y M, Ma Z, Ahmad F, Syed T N, Shaikh S A, et al . Influence of moisture content and compressive loading speed on the mechanical properties of maize grain orientations. Int J Agric & Biol Eng, 2021; 14(5): 41–49.

[31] Di Z F, Cui Z K, Zhang H, Zhou J, Zhang M Y, Bu L X. Design and experiment of rasp bar and nail tooth combined axial flow corn threshing cylinder. Transactions of CSAE, 2018; 34(1): 28–34. (in Chinese)

[32] Wang Z B, Wang Z W, Zhang Y P, Yan W X, Chi Y J, Liu C Q. Design and test of longitudinal axial flexible hammer-calw corn thresher. Transaction of CASE, 2020; 51(S2): 109–117. (in Chinese)